

# What is the Pairing Glue in the Cuprates? Insights from Normal and Anomalous Propagators

T. Bzdušek<sup>a,b</sup> and R. Hlubina<sup>a†</sup>

<sup>a</sup>*Department of Experimental Physics, Comenius University, Mlynská Dolina F2,  
842 48 Bratislava, Slovakia;* <sup>b</sup>*Theoretische Physik, ETH-Hönggerberg, CH-8093 Zürich,  
Switzerland*

(January 2014)

Both the pairing and the pair-breaking modes lead to similar kinks of the electron dispersion curves in superconductors, and therefore the photoemission spectroscopy can not be straightforwardly applied in search for their pairing glue. If the momentum-dependence of the normal and anomalous self-energy can be neglected, manipulation with the data does allow us to extract the gap function  $\Delta(\omega)$  and therefore also the pairing glue. However, in the superconducting cuprates such procedure may not be justified. In this paper we point out that the pairing glue is more directly visible in the spectral function of the Nambu-Gor'kov anomalous propagator and we demonstrate that this function is in principle experimentally observable.

**Keywords:** superconducting cuprates; pairing glue; pair-breaking modes; anomalous propagator; spectral functions

## 1. Introduction

Although the nature of the normal state of the cuprates remains enigmatic, their superconducting state is generally believed to be quite conventional [1]. In fact, superconductivity of the cuprates is a consequence of the global  $U(1)$  symmetry breaking caused by Cooper-pair condensation, i.e. by the same mechanism as in the conventional low- $T_c$  superconductors. The Cooper pairs are formed by electrons in a single  $\text{CuO}_2$  plane and their spin is  $S = 0$ . A minor modification is that the orbital wave-function of the Cooper pairs transforms as the so-called  $d$ -wave under the point group of the  $\text{CuO}_2$  plane. The major open question of the cuprate physics is what forms the pairing glue which holds the electrons in the Cooper pairs together, or even whether such a pairing glue is present at all [2].

If we introduce the Nambu spinors  $\alpha_{\mathbf{k}}^\dagger = (c_{\mathbf{k}\uparrow}^\dagger, c_{-\mathbf{k}\downarrow})$ , all single-particle properties of the cuprates should be described by the Nambu-Gor'kov Green's function  $\mathcal{G}_{\mathbf{k}}(\tau) = -\langle T\alpha_{\mathbf{k}}(-i\tau)\alpha_{\mathbf{k}}^\dagger \rangle$  [see, e.g., 3]. Note that we work in the imaginary-time formalism and that  $\mathcal{G}_{\mathbf{k}}(\tau)$  is a  $2 \times 2$  matrix

$$\mathcal{G}_{\mathbf{k}}(\tau) = \begin{pmatrix} G_{\mathbf{k}\uparrow}(\tau) & F_{\mathbf{k}\uparrow}(\tau) \\ F_{\mathbf{k}\uparrow}^*(\tau) & -G_{-\mathbf{k}\downarrow}(-\tau) \end{pmatrix},$$

which is determined by two functions: by the diagonal Green's function (normal

<sup>†</sup>This is an Author's Original Manuscript of an article submitted for consideration in the Philosophical Magazine ©Taylor & Francis; Philosophical Magazine is available online at <http://www.tandfonline.com/loi/tphm20>.

propagator)  $G_{\mathbf{k}\sigma}(\tau) = -\langle T c_{\mathbf{k}\sigma}(-i\tau) c_{\mathbf{k}\sigma}^\dagger \rangle$ , as well as by the off-diagonal Green's function (anomalous propagator)  $F_{\mathbf{k}\sigma}(\tau) = -\langle T c_{\mathbf{k}\sigma}(-i\tau) c_{-\mathbf{k}-\sigma} \rangle$ . We emphasize that the Green's function  $\mathcal{G}_{\mathbf{k}}(\tau)$  may be introduced even if the Landau-BCS Fermi liquid theory does not apply to the cuprates.

The spectral representation of the Green's function is defined as:

$$\mathcal{G}_{\mathbf{k}}(i\omega_l) = \int_{-\infty}^{\infty} \frac{dx \mathcal{A}_{\mathbf{k}}(x)}{i\omega_l - x}, \quad \mathcal{A}_{\mathbf{k}}(x) = \begin{pmatrix} A_{\mathbf{k}\uparrow}(x) & B_{\mathbf{k}\uparrow}(x) \\ B_{\mathbf{k}\uparrow}^*(x) & A_{-\mathbf{k}\downarrow}(-x) \end{pmatrix}, \quad (1)$$

where we have introduced the spectral function of the normal propagator  $A_{\mathbf{k}\sigma}(x)$ , as well as the spectral function of the anomalous propagator  $B_{\mathbf{k}\sigma}(x)$ . In the Lehmann representation, these functions read as

$$A_{\mathbf{k}\sigma}(x) = (1 + e^{-x/T}) \frac{1}{Z} \sum_{m,n} e^{-E_m/T} \left| \langle m | c_{\mathbf{k}\sigma}^\dagger | n \rangle \right|^2 \delta(x - E_n + E_m),$$

$$B_{\mathbf{k}\sigma}(x) = (1 + e^{-x/T}) \frac{1}{Z} \sum_{m,n} e^{-E_m/T} \langle m | c_{\mathbf{k}\sigma} | n \rangle \langle n | c_{-\mathbf{k}-\sigma} | m \rangle \delta(x - E_n + E_m),$$

where  $T$  is the temperature. Throughout this paper we set  $k_B = 1$  and  $\hbar = 1$ .

In singlet superconductors with even parity we expect that  $A_{\mathbf{k}\uparrow}(x) = A_{\mathbf{k}\downarrow}(x) = A_{\mathbf{k}}(x)$  and  $A_{\mathbf{k}}(x) = A_{-\mathbf{k}}(x)$ . For the same reason, we expect that  $B_{\mathbf{k}\uparrow}(x) = -B_{\mathbf{k}\downarrow}(x) = B_{\mathbf{k}}(x)$  and  $B_{\mathbf{k}}(x) = B_{-\mathbf{k}}(x)$ . When combined with the property  $B_{\mathbf{k}\sigma}(x) = B_{-\mathbf{k}-\sigma}(-x)$  which follows from hermiticity, we finally find that the anomalous spectral function is odd,  $B_{\mathbf{k}}(x) = -B_{\mathbf{k}}(-x)$ .

Note that the normal spectral function  $A_{\mathbf{k}}(x)$  is real and positive, therefore allowing for a probabilistic interpretation. It is this function which is measured in the angle-resolved photoemission experiments (ARPES) [4]. Moreover, the integral  $N_S(x) = \frac{1}{V} \sum_{\mathbf{k}} A_{\mathbf{k}}(x)$ , where  $V$  is the normalisation volume, is directly accessible in the tunneling experiments [3].

On the other hand, the function  $B_{\mathbf{k}}(x)$  is in general complex and therefore it does not have an obvious probabilistic interpretation. Moreover,  $B_{\mathbf{k}}(x)$  depends on the phase of the condensate. At the present time there seem to be no established experimental procedures which would determine the function  $B_{\mathbf{k}}(x)$ .

Thus only one of the two functions  $A_{\mathbf{k}}(x)$  and  $B_{\mathbf{k}}(x)$ , which are needed to characterize the single-particle properties of a superconductor, is currently experimentally accessible. In Section 2 we show that, even in conventional superconductors where the electrons interact via exchange of bosonic interactions, this lack of information may lead to severe errors in identifying the pairing glue by ARPES. We demonstrate that both, the pairing and the pair-breaking interactions, modify the normal spectral function  $A_{\mathbf{k}}(x)$  in essentially the same way, making them indistinguishable in a naive  $A_{\mathbf{k}}(x)$ -based experiment. A similar observation has been made very recently in the context of the cuprates [5]: the magnitude of the dispersion kink at 70 meV in  $\text{La}_{2-x}\text{Sr}_x\text{CuO}_4$  has been found to decrease by only 30% between the superconducting sample with  $x = 0.20$  and  $T_c = 32$  K and a non-superconducting overdoped sample with  $x = 0.30$  and  $T_c = 0$  K. From here the authors conclude that these dispersion kinks can not be caused by the pairing glue of superconductivity.

Within the Eliashberg theory, the two functions  $A_{\mathbf{k}}(x)$  and  $B_{\mathbf{k}}(x)$  are encoded in two functions  $Z_{\mathbf{k}}(\omega)$  and  $\Delta_{\mathbf{k}}(\omega)$ . In Section 3 we show that, under certain simplifying assumptions which happen to be satisfied in the conventional superconductors, the function  $\Delta_{\mathbf{k}}(\omega)$  which characterizes the pairing can be quite unexpectedly extracted from the measurement of only  $A_{\mathbf{k}}(x)$ . In Section 3 we also describe some

recent attempts to apply this type of approach to the cuprate superconductors.

Finally, in Section 4 we go beyond the  $A_{\mathbf{k}}(x)$ -based spectroscopic techniques and we suggest how, at least in principle, the anomalous spectral function  $B_{\mathbf{k}}(x)$  can be determined directly from the current-current correlation function of the Josephson junctions.

## 2. Eliashberg theory: pairing vs. pair-breaking modes

The Eliashberg theory [3] results from a combination of the Dyson equation  $\mathcal{G}_{\mathbf{k}}(i\omega_n) = \left[ i\omega\tau_0 - \varepsilon_k\tau_3 - \hat{\Sigma}_{\mathbf{k}}(i\omega_n) \right]^{-1}$  with a self-consistent Born approximation for the  $2 \times 2$  self-energy matrix  $\hat{\Sigma}_{\mathbf{k}}(i\omega)$ . In the electron-phonon case, this is virtually exact due to the Migdal “theorem”. For the sake of simplicity, let us assume that the system under study is isotropic and particle-hole symmetric. Then we can make the following ansatz for the self-energy of an  $s$ -wave pairing state:  $\hat{\Sigma}_{\mathbf{k}}(i\omega_n) = (1 - Z_n)i\omega_n\tau_0 + \Delta_n Z_n\tau_1$ , where the wave-function renormalisation  $Z_n = Z(i\omega_n)$  and the gap function  $\Delta_n = \Delta(i\omega_n)$  are real functions (only) of frequency,  $\tau_0$  is a  $2 \times 2$  unit matrix, and  $\tau_i$  with  $i = 1, 2, 3$  are the Pauli matrices. The diagonal and off-diagonal components of the resulting Green’s function in this simple case read as

$$G_{\mathbf{k}}(i\omega_n) = -\frac{i\omega_n Z_n + \varepsilon_k}{Z_n^2(\omega_n^2 + \Delta_n^2) + \varepsilon_k^2}, \quad F_{\mathbf{k}}(i\omega_n) = -\frac{Z_n \Delta_n}{Z_n^2(\omega_n^2 + \Delta_n^2) + \varepsilon_k^2}. \quad (2)$$

In order to illustrate the difference between the pairing and pair-breaking modes, let us consider the following simple model of interacting electrons and bosons:

$$H_{\text{int}} = \frac{1}{\sqrt{V}} \sum_{\mathbf{q} \neq 0} [g_{0\mathbf{q}} \rho_{\mathbf{q}} A_{-\mathbf{q}}^0 + g_{\perp\mathbf{q}} \mathbf{j}_{\mathbf{q}} \cdot \mathbf{A}_{-\mathbf{q}}]. \quad (3)$$

The first term describes the coupling of strength  $g_{0\mathbf{q}}$  between the electron charge density  $\rho_{\mathbf{q}} = \sum_{\mathbf{k}\sigma} c_{\mathbf{k}-\mathbf{q}/2\sigma}^\dagger c_{\mathbf{k}+\mathbf{q}/2\sigma}$  and a scalar mode with the propagator  $D_0(\mathbf{q}, \tau) = \langle T A_{-\mathbf{q}}^0(-i\tau) A_{\mathbf{q}}^0 \rangle$  and the Fourier transform  $D_0(\mathbf{q}, \omega_n)$ . The second term describes the coupling of strength  $g_{\perp\mathbf{q}}$  between the electron current density  $\mathbf{j}_{\mathbf{q}} = \frac{1}{k_F} \sum_{\mathbf{k}\sigma} \mathbf{k} c_{\mathbf{k}-\mathbf{q}/2\sigma}^\dagger c_{\mathbf{k}+\mathbf{q}/2\sigma}$  and a vector mode with the propagator  $D_{ij}(\mathbf{q}, \tau) = \langle T A_{-\mathbf{q}}^i(-i\tau) A_{\mathbf{q}}^j \rangle$  and the Fourier transform  $D_{ij}(\mathbf{q}, \omega_n) = D_{\perp}(\mathbf{q}, \omega_n) (\delta_{ij} - q_i q_j / q^2)$ . In the Nambu representation we can write

$$\rho_{\mathbf{q}} = \sum_{\mathbf{k}} \alpha_{\mathbf{k}-\mathbf{q}/2}^\dagger \tau_3 \alpha_{\mathbf{k}+\mathbf{q}/2}, \quad \mathbf{j}_{\mathbf{q}} = \frac{1}{k_F} \sum_{\mathbf{k}} \mathbf{k} \alpha_{\mathbf{k}-\mathbf{q}/2}^\dagger \tau_0 \alpha_{\mathbf{k}+\mathbf{q}/2}.$$

The presence of different  $\tau$ -matrices in  $\rho_{\mathbf{q}}$  and  $\mathbf{j}_{\mathbf{q}}$  is caused by the different behaviour of charge and current under time reversal. In the self-consistent Born approximation, the  $2 \times 2$  self-energy matrix corresponding to  $H_{\text{int}}$  is given by

$$\begin{aligned} \hat{\Sigma}_{\mathbf{k}}(i\omega_n) &= \frac{T}{V} \sum_{\mathbf{k}'\omega_m} g_{0\mathbf{k}'-\mathbf{k}}^2 D_0(\mathbf{k}' - \mathbf{k}, \omega_m - \omega_n) \tau_3 \mathcal{G}_{\mathbf{k}'}(i\omega_m) \tau_3 \\ &+ \frac{T}{V} \sum_{\mathbf{k}'\omega_m} \frac{(\mathbf{k} \times \mathbf{k}')^2}{k_F^2 (\mathbf{k}' - \mathbf{k})^2} g_{\perp\mathbf{k}'-\mathbf{k}}^2 D_{\perp}(\mathbf{k}' - \mathbf{k}, \omega_m - \omega_n) \tau_0 \mathcal{G}_{\mathbf{k}'}(i\omega_m) \tau_0. \end{aligned}$$

For the sake of simplicity, in what follows let us replace the factor  $\frac{(\mathbf{k} \times \mathbf{k}')^2}{k_F^2 (\mathbf{k}' - \mathbf{k})^2}$  by its value for forward scattering, i.e. by 1. Performing furthermore the radial integrations in the usual way by introducing the electronic density of states in the normal state  $N(0)$ , the Eliashberg equations reduce to the standard form

$$Z_n = 1 + \frac{\pi T}{\omega_n} \sum_m \sum_{s=0,\perp} g_s(\omega_n - \omega_m) \frac{\omega_m}{\sqrt{\omega_m^2 + \Delta_m^2}}, \quad (4a)$$

$$Z_n \Delta_n = \pi T \sum_m \sum_{s=0,\perp} \eta_s g_s(\omega_n - \omega_m) \frac{\Delta_m}{\sqrt{\omega_m^2 + \Delta_m^2}}, \quad (4b)$$

where  $g_s(\omega_n) = \frac{1}{2} N(0) \overline{g_s^2 D_s(\omega_n)}$  are dimensionless coupling functions for the two modes  $s = 0, \perp$  and  $\overline{g_s^2 D_s(\omega_n)}$  is a Fermi-surface average of  $g_{s\mathbf{k}'-\mathbf{k}}^2 D_s(\mathbf{k}' - \mathbf{k}, \omega_n)$ .

Note that both modes enter equation (4a) for the wave-function renormalisation in a symmetric way. This is not the case, however, for equation (4b) for the gap function, since  $\eta_0 = 1$  and  $\eta_\perp = -1$ , clearly distinguishing the pairing scalar mode from the pair-breaking vector mode. This difference is caused by the difference in  $\tau$ -matrices, i.e. by the different behaviour of charge and current under time reversal. Physically, the result  $\eta_\perp = -1$  is a consequence of the repulsive force between antiparallel currents carried by the electrons forming a Cooper pair.

It is worth pointing out that the Eliashberg equations (4) can be generalized to take into account also finite impurity scattering treated within the self-consistent Born approximation, if we include an additional scattering mode  $s = \text{imp}$  with an elastic coupling function  $g_{\text{imp}}(\omega_n) = \frac{\Gamma_{\text{imp}}}{\pi T} \delta_{n0}$  and  $\eta_{\text{imp}} = 1$ . Also a simplified version of pair-breaking elastic scattering on the magnetic impurities can be described by the same formalism by including yet another scattering mode  $s = \text{mag}$  with the coupling function  $g_{\text{mag}}(\omega_n) = \frac{\Gamma_{\text{mag}}}{\pi T} \delta_{n0}$  and  $\eta_{\text{mag}} = -1$ .

In Figure 1 we plot the wave-function renormalisation and the gap function, after analytical continuation to the real axis by means of the Padé approximation [6], for the two-mode model (3). We have considered coupling to Debye-type modes with coupling strengths  $g_{s\mathbf{q}} \propto \sqrt{q}$  and linear dispersions  $\omega_s(q) = v_s q$ , which leads to the coupling functions  $g_s(\omega_n) = \lambda_s \left[ 1 - \frac{\omega_n^2}{\Omega_s^2} \ln \left( 1 + \frac{\Omega_s^2}{\omega_n^2} \right) \right]$  with dimensionless coupling constants  $\lambda_s$  and characteristic frequencies  $\Omega_s$ . The crucial observation to be made in Figure 1 is that the wave-function renormalisation  $Z(\omega)$  does not distinguish between pairing and pair-breaking modes: for instance, at both characteristic frequencies  $\Omega_0$  and  $\Omega_\perp$ , the imaginary part  $Z''(\omega)$  exhibits local maxima. Whether we are dealing with a pairing or a pair-breaking mode is visible only in the gap function  $\Delta(\omega)$ . In fact, for  $\omega > 0$  the imaginary part  $\Delta''(\omega)$  exhibits a local minimum close to the pair-breaking scale  $\Omega_\perp$ , while close to the pairing scale  $\Omega_0$  it exhibits a maximum. Similarly, when we lower the energy  $\omega$  below  $\Omega_0$ , the pairing energy  $\Delta'(\omega)$  increases, while exactly opposite behaviour is observed in the vicinity of  $\Omega_\perp$ .

The same dichotomy is observed also in the language of spectral functions: the normal spectral function  $A_{\mathbf{k}}(x)$  does not distinguish the pairing from the pair-breaking modes, since it exhibits maxima in the vicinity of both,  $\Omega_0$  and  $\Omega_\perp$ . On the contrary, the anomalous spectral function  $B_{\mathbf{k}}(x)$  exhibits for  $x > 0$  local maxima in the vicinity of the pair-breaking energy  $\Omega_\perp$ , whereas local minima are observed close to the pairing energy  $\Omega_0$ .

Note that in the gauge which we have chosen to work in,  $B_{\mathbf{k}}(x)$  is real but not positive even if we restrict ourselves to  $x > 0$ . The necessity of a sign change of

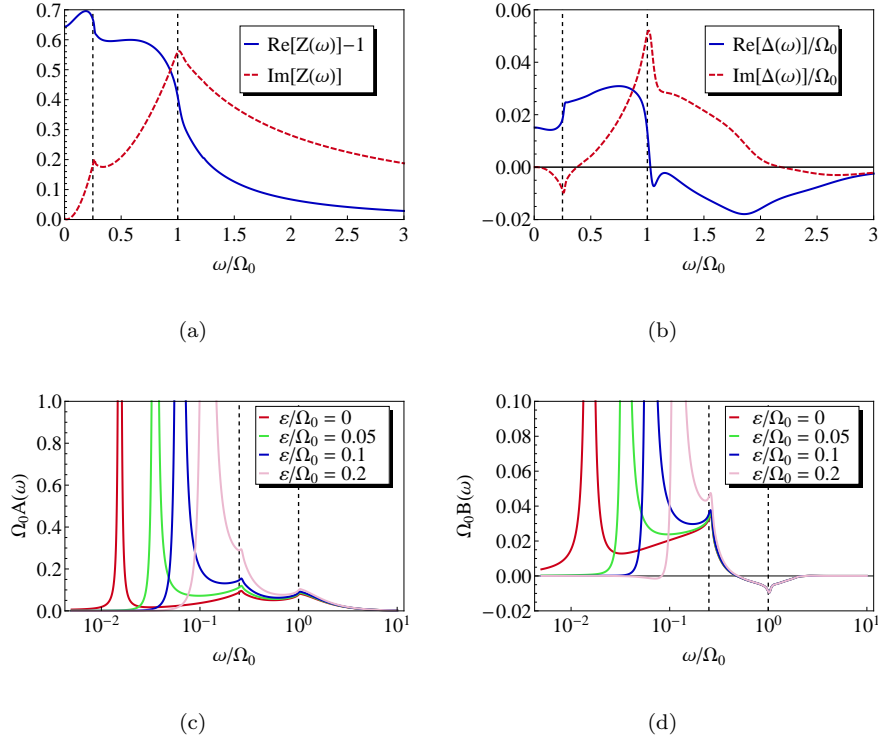


Figure 1. (colour online) Real and imaginary parts of the wave-function renormalisation  $Z(\omega) = Z'(\omega) + iZ''(\omega)$  (a) and of the gap function  $\Delta(\omega) = \Delta'(\omega) + i\Delta''(\omega)$  (b) for the two-mode model (3) with a pairing mode with dimensionless coupling  $\lambda_0 = 0.5$  and frequency  $\Omega_0$ , and a pair-breaking mode with  $\lambda_\perp = 0.15$  and  $\Omega_\perp = 0.25\Omega_0$ . The critical temperature of the model is  $T_c \approx 0.009\Omega_0$ . The results were obtained by analytic continuation of data obtained on the imaginary axis at temperature  $T = 0.005\Omega_0$ . The dotted lines show the energy scales  $\Omega_0$  and  $\Omega_\perp$ . Panels (c,d) show the energy distribution curves at  $\omega > 0$  of the normal and anomalous spectral functions determined from the data in panels (a,b) at fixed values of  $\varepsilon_k$  (left to right curves correspond to increasing  $\varepsilon_k$ ). Note the logarithmic scale of  $\omega$ .

$B_{\mathbf{k}}(x)$  follows from the following exact sum rule which we prove in Appendix A:

$$\int_{-\infty}^{\infty} dx x B_{\mathbf{k}}(x) = 2 \int_0^{\infty} dx x B_{\mathbf{k}}(x) = 0. \quad (5)$$

It is worth pointing out that if the Coulomb pseudopotential  $\mu^*$  is included in equations (4) then the sum rule (5) does not hold any more, but we have checked that the function  $B_{\mathbf{k}}(x)$  still exhibits both, a sign change and a feature close to the energy of the pairing glue.

### 3. Eliashberg theory: determination of the gap function

#### 3.1. Tunneling density of states

It is well known that the tunneling experiments gave the historically first direct access to the gap function  $\Delta(\omega)$  of the conventional superconductors [7]. It is rarely stressed, however, that the very possibility to interpret the tunneling density of states  $N_S(\omega)$  solely in terms of  $\Delta(\omega)$  is somewhat surprising. In fact,  $N_S(\omega)$  per

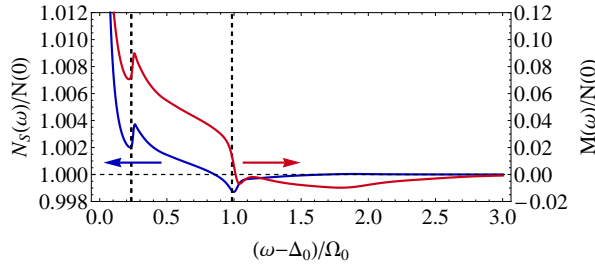


Figure 2. (colour online) Tunneling density of states  $N_S(\omega)$  and anomalous density of states  $M(\omega)$  for the two-mode model (3). The parameters are the same as in Fig. 1. Note the structure close to the energy scales  $\Omega_0$  and  $\Omega_\perp$  (which are shown by the dotted lines).

spin is given by

$$N_S(\omega) = \frac{1}{V} \sum_{\mathbf{k}} A_{\mathbf{k}}(\omega) \approx -\frac{1}{\pi} N(0) \int d\varepsilon_k \text{Im} G_{\mathbf{k}}(\omega + i0), \quad (6)$$

where in the approximate equality we have assumed that the system is effectively isotropic, and that the density of states in the normal state does not vary appreciably on the energy scale of the superconducting gap. The surprise has to do with the fact that  $G_{\mathbf{k}}(\omega)$  is given by equation (2), that is by two functions  $Z_{\mathbf{k}}(\omega)$  and  $\Delta_{\mathbf{k}}(\omega)$  in the general case. But it should not be possible to determine *two* functions from a measurement of a *single* function  $N_S(\omega)$ ! The solution to this paradox is that, if  $Z_{\mathbf{k}}(\omega)$  and  $\Delta_{\mathbf{k}}(\omega)$  do not depend on  $\mathbf{k}$ , the integration over  $\varepsilon_k$  can be performed and it leads to the result (assuming that the branch cut of the square root is set along the negative real axis)

$$\frac{N_S(\omega)}{N(0)} \approx \text{Re} \frac{|\omega|}{\sqrt{\omega^2 - \Delta^2(\omega)}}, \quad (7)$$

which does not depend on  $Z(\omega)$  any more. Therefore (7) can be used as a tool for measuring the gap function  $\Delta(\omega)$ . It should be pointed out that the inversion of the formula (7) is not completely trivial, since  $\Delta(\omega) = \Delta'(\omega) + i\Delta''(\omega)$  is a complex function, but thanks to the analytic properties of  $\Delta(\omega)$  it can be performed [8].

In Figure 2 we plot the tunneling density of states  $N_S(\omega)$  for the two-mode model (3). We have introduced the spectral gap  $\Delta_0$  as a solution to the equation  $\omega = \Delta'(\omega)$  and we find  $\Delta_0 = 0.015\Omega_0$ . Note that  $N_S(\omega)$  exhibits local increase at the pair-breaking scale  $\Omega_\perp + \Delta_0$  and a decrease at the pairing scale  $\Omega_0 + \Delta_0$ .

### 3.2. Tomographic density of states

The pairing state within a  $\text{CuO}_2$  plane is known to be anisotropic [1], therefore the results for the density of states derived in Section 3.1 obviously do not apply to the cuprates. In order to account for their in-plane anisotropy, let us introduce the curvilinear coordinates  $\mathbf{k} = (k_\parallel, k_\perp)$ , where  $k_\parallel$  varies along the Fermi line and  $k_\perp$  varies along the normal to the Fermi line. Let us further denote the length of the Fermi line as  $\oint dk_\parallel = 2\pi k_F$  and instead of  $k_\parallel$  define the angular variable  $\theta$  along the Fermi line by  $d\theta = dk_\parallel/k_F$ . Let us also replace the coordinate  $k_\perp$  by the non-interacting energy  $\varepsilon_k$ , making use of the relation  $d\varepsilon_k = v_F(\theta)dk_\perp$ , where  $v_F(\theta)$  is the Fermi velocity at angle  $\theta$ .

The functions  $Z_{\mathbf{k}}(\omega)$  and  $\Delta_{\mathbf{k}}(\omega)$  entering the definition of the Green's function (2) depend in general on three variables  $(\varepsilon_k, \theta, \omega)$ . If we now assume, in analogy with

conventional superconductors, that their dependence on  $\varepsilon_k$  can be neglected, then the  $\varepsilon_k$ -integration in equation (6) can be performed and we arrive at the expression for the two-dimensional density of states per spin

$$N_S(\omega) = \frac{k_F}{(2\pi)^2} \oint d\theta N_S(\theta, \omega), \quad (8)$$

where we have defined the angle-resolved (tomographic) density of states

$$N_S(\theta, \omega) = \int_{\theta=\text{const}} dk_{\perp} A_{\mathbf{k}}(\omega) = \frac{1}{v_F(\theta)} \text{Re} \frac{|\omega|}{\sqrt{\omega^2 - \Delta^2(\theta, \omega)}}. \quad (9)$$

Usually it is assumed that scanning tunneling spectroscopy from the  $c$ -axis direction gives us direct access to the tunneling density of states  $N_S(\omega)$  in the cuprates [9]. However, even if we assume that equations (8,9) do apply, their direct inversion with the goal of determining  $\Delta(\theta, \omega)$  is not possible, due to the  $\theta$ -dependence of the gap function. The best one can do is to fit the data for  $N_S(\omega)$  to a postulated microscopic model and to extract the relevant parameters in this way. A recent example of such a procedure can be found in [9], where the tunneling data on Bi2223 have been fit to a phenomenological model with spin-fluctuation induced pairing. It should be pointed out, however, that no less than 13 parameters were needed in the fits. Clearly, a less biased technique for determination of  $\Delta(\theta, \omega)$  is needed.

Very recently, it has been realized [10, 11] that the tomographic density of states can be determined from the ARPES data by taking their integral according to the definition (9). Very promising results for  $N_S(\theta, \omega)$  have been found for angles  $\theta$  lying close to the nodal direction. Since the authors were interested only in the simplest questions regarding the interplay between the pair-breaking rate  $\Gamma(\theta)$  and the gap magnitude  $\Delta(\theta)$ , the measured tomographic density of states was fitted to the Dynes formula. However, by applying the powerful inversion technology [8] to the data for  $N_S(\theta, \omega)$  at fixed angle  $\theta$ , it should be possible to obtain the full complex function  $\Delta(\theta, \omega) = \Delta'(\theta, \omega) + i\Delta''(\theta, \omega)$  without making any additional assumptions about its shape. This might open an unbiased way to the identification of the pairing glue in the cuprates.

### 3.3. Anomalous branch of the momentum distribution curves

Let us assume again that the functions  $Z(\theta, \omega)$  and  $\Delta(\theta, \omega)$  depend only on  $\theta$  and  $\omega$ , but not on  $\varepsilon_k$ . ARPES measures the spectral function

$$A(\varepsilon_k, \theta, \omega) = -\frac{1}{\pi} \text{Im} \left[ \frac{\omega Z(\theta, \omega) + \varepsilon_k}{\omega^2 Z(\theta, \omega)^2 - \phi(\theta, \omega)^2 - \varepsilon_k^2} \right], \quad (10)$$

where  $\phi(\theta, \omega) = Z(\theta, \omega)\Delta(\theta, \omega)$  is the anomalous self-energy. It is well established [4] that, in the normal state and in absence of a gap, the spectral function  $A(\varepsilon_k, \theta, \omega)$  of the cuprates exhibits a simple Lorentzian peak when plotted as a function of  $\varepsilon_k$  at fixed values of  $\omega$  and  $\theta$ . Such plots are called momentum distribution functions and their simple shape can be taken as an a posteriori evidence for independence of  $Z(\theta, \omega)$  on  $\varepsilon_k$  [4]. Moreover, if the bare dispersion  $\varepsilon_k$  is known, then the function  $Z(\theta, \omega) = Z'(\theta, \omega) + iZ''(\theta, \omega)$  can be easily determined by fitting the momentum distribution functions to a Lorentzian.

Let us generalize the predictions of equation (10) for the momentum distribution function to the superconducting state. To illustrate the point, let us consider the

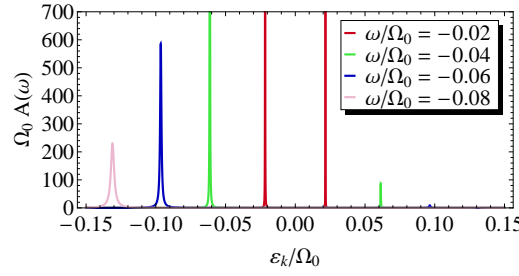


Figure 3. (colour online) Momentum distribution curves for the two-mode model (3). The parameters are the same as in Fig. 1. The curves consist of two peaks placed symmetrically around the Fermi surface  $\varepsilon_k = 0$ . Their distance from  $\varepsilon_k = 0$  increases with increasing  $|\omega|$ .

simplest case with real  $Z(\theta, \omega)$  and  $\Delta(\theta, \omega)$ . In that case we find

$$A(\varepsilon_k, \theta, \omega) = \frac{|\omega| + \text{sgn}(\omega)\Omega}{2\Omega} \delta(\varepsilon_k - Z\Omega) + \frac{|\omega| - \text{sgn}(\omega)\Omega}{2\Omega} \delta(\varepsilon_k + Z\Omega),$$

where  $\Omega(\theta, \omega) = \sqrt{\omega^2 - \Delta^2(\theta, \omega)}$ . This result shows, as is well known, that excitations with a given energy  $\omega$  are realized at two momenta: one inside and another one outside the Fermi sea, corresponding to  $\varepsilon_k = \pm Z(\theta, \omega)\Omega(\theta, \omega)$ . If only one of the branches is observable, then the measurement of the quasiparticle dispersion can not be inverted to obtain the function  $\Delta(\theta, \omega)$ , since the wave-function renormalisation  $Z(\theta, \omega)$  is unknown. However, if both branches are observable, then the additional information on the relative weight of the two branches allows us to determine  $\Omega(\theta, \omega)$ , and, as a consequence, both  $\Delta(\theta, \omega)$  and  $Z(\theta, \omega)$  can be determined.

In a sense, the observation of the two branches gives us two independent measurements which enable the determination of the two independent functions  $\Delta(\theta, \omega)$  and  $Z(\theta, \omega)$ . This idea has been used very recently in an interesting paper [12], where the momentum distribution curves for a set of angles  $\theta$  have been studied on a fine grid of energies  $\omega < 0$ . At fixed  $\omega$  and  $\theta$ , the data was fitted to equation (10), making use of 4 parameters describing the real and imaginary parts of the wave-function renormalisation  $Z = Z' + iZ''$  as well as of the anomalous self-energy  $\phi = \phi' + i\phi''$ . For technical reasons, two additional fitting parameters had to be used: one for the overall intensity, and another one for background subtraction. The bare dispersion  $\varepsilon_k$  was taken from a tight-binding model.

The momentum distribution curves for the two-mode model (3) for several values of  $\omega$  are shown in Figure 3. Note that the anomalous branch has substantial weight only for those energies  $\omega$ , for which  $|\omega| \sim \Delta_0$ . For larger values of  $|\omega|$ , the results for the anomalous self-energy necessarily become quite noisy, as in fact found also in [12]. Therefore this technique is potentially useful in cases where the characteristic energy of the pairing glue is comparable to the energy gap.

#### 4. Direct measurement of the anomalous spectral function

All of the techniques for determination of the gap function  $\Delta_{\mathbf{k}}(\omega)$  described in Section 3 were based on the measurement of the diagonal spectral function  $A_{\mathbf{k}}(x)$ . The crucial feature which had to be assumed was that the functions  $\Delta(\varepsilon_k, \theta, \omega)$  and  $Z(\varepsilon_k, \theta, \omega)$  do not depend on  $\varepsilon_k$ . While this assumption is well established in the context of low-temperature superconductors, it is far from obvious that it applies to the cuprates as well. On one hand, the simplicity of the momentum distribution curves as opposed to the complicated energy distribution curves in



ARPES can be taken as indirect evidence for such weak  $\varepsilon_k$ -dependence [4]. But on the other hand, since the cuprates are doped Mott insulators, one should expect large particle-hole asymmetry, and therefore also strong  $\varepsilon_k$ -dependence, as in fact observed in tunneling experiments [13]. Also the more standard concept of spin-fluctuation mediated superconductivity naturally leads to a strong  $\varepsilon_k$ -dependence, because only at the hot spots the scattering is equally strong for electron states inside and outside the Fermi sea. Away from the hot spots, scattering either inside or outside the Fermi sea should dominate, depending on the angle  $\theta$ .

An obvious recipe to determine the *two functions*  $\Delta_{\mathbf{k}}(\omega)$  and  $Z_{\mathbf{k}}(\omega)$  is to measure the *two spectral functions* characterizing a superconductor, namely  $A_{\mathbf{k}}(x)$  and  $B_{\mathbf{k}}(x)$ . We are thus led to the search for a suitable spectroscopic technique for the anomalous spectral function  $B_{\mathbf{k}}(x)$ . A natural candidate is the Josephson effect, where the Cooper pairs enter or leave a given superconductor. However, the Josephson current is determined by an integral of  $B_{\mathbf{k}}(x)$ , providing just one number and not a function of a continuous parameter, needed for a spectroscopic measurement. We are therefore led to the study of the frequency spectrum of temporal fluctuations of the current  $I(t)$  traversing the Josephson junction at zero bias  $S(\omega) = \int_{-\infty}^{\infty} dt \langle I(t)I(0) \rangle e^{i\omega t}$  or, making use of the fluctuation-dissipation theorem  $S(\omega) = -2[n(\omega) + 1]\chi''(\omega)$ , of the retarded current-current correlation function

$$\chi(\omega) = -i \int_{-\infty}^{\infty} dt e^{i(\omega+i0)t} \langle [I(t), I(0)] \rangle \theta(t). \quad (11)$$

In what follows we calculate  $\chi''(\omega)$  for a Josephson junction between two superconductors, which we call left and right. Let us denote the single-particle states of the left and right superconductors by  $\mathbf{k}$  and  $\mathbf{q}$ , respectively. If we describe the junction by the tunneling Hamiltonian  $H_{\text{tun}} = \sum_{\mathbf{kq}} [t_{\mathbf{kq}}(c_{\mathbf{k}\uparrow}^\dagger c_{\mathbf{q}\uparrow} + c_{-\mathbf{q}\downarrow}^\dagger c_{-\mathbf{k}\downarrow}) + \text{h.c.}]$ , the current operator is given by  $I = -ie \sum_{\mathbf{kq}} [t_{\mathbf{kq}} \alpha_{\mathbf{k}}^\dagger \alpha_{\mathbf{q}} - \text{h.c.}]$ . A simple evaluation of (11) to second order in the tunneling matrix element gives

$$\chi''(\omega) = 2\pi e^2 \sum_{\mathbf{kq}} |t_{\mathbf{kq}}|^2 \int_{-\infty}^{\infty} dx [f(x+\omega) - f(x)] [A_{\mathbf{kq}}(x, \omega) + B_{\mathbf{kq}}(x, \omega)], \quad (12)$$

where  $A_{\mathbf{kq}}(x, \omega) = A_{\mathbf{k}}(x)A_{\mathbf{q}}(x+\omega) + A_{\mathbf{k}}(-x)A_{\mathbf{q}}(-x-\omega)$  generates the normal contribution  $\chi_N''(\omega)$  and  $B_{\mathbf{kq}}(x, \omega) = B_{\mathbf{k}}(x)B_{\mathbf{q}}^*(x+\omega) + B_{\mathbf{k}}^*(x)B_{\mathbf{q}}(x+\omega)$  generates the superconducting contribution  $\chi_S''(\omega)$ .

If we drive one of the superconductors forming the junction into its normal state, e.g. by applying magnetic field or by heating above  $T_c$ , we can determine the normal contribution  $\chi_N''(\omega)$  and therefore isolate the superconducting contribution  $\chi_S''(\omega) = \chi''(\omega) - \chi_N''(\omega)$ . Alternatively, we can study the current fluctuations around a finite supercurrent stabilized by a phase difference  $\phi$  between the electrodes. In that case we find  $\chi_S''(\omega) = \chi_{S0}''(\omega) \cos \phi$ , where

$$\chi_{S0}''(\omega) = 4\pi e^2 \sum_{\mathbf{kq}} |t_{\mathbf{kq}}|^2 \int_{-\infty}^{\infty} dx [f(x+\omega) - f(x)] B_{\mathbf{k}}(x)B_{\mathbf{q}}(x+\omega),$$

and the anomalous spectral functions are calculated in a gauge where both superconductors have a real order parameter. Measuring the component of  $S(\omega)$  proportional to  $\cos \phi$ , we can therefore directly measure  $\chi_{S0}''(\omega)$ .

In order to proceed, let us further assume that the tunneling is featureless,  $|t_{\mathbf{kq}}|^2 = |t|^2 \mathcal{S}/\mathcal{V}^2$ , where  $\mathcal{S}$  is the junction area and  $\mathcal{V}$  is the normalisation vol-

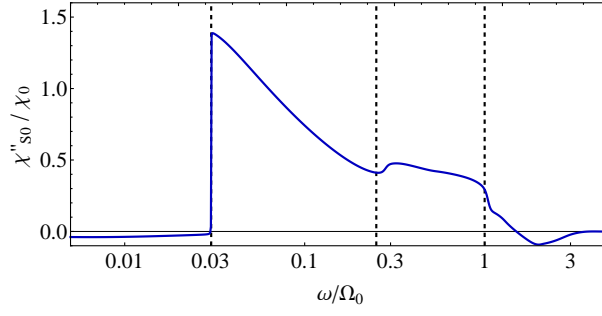


Figure 4. (colour online) The current-current correlation function  $\chi''_{S0}(\omega)$  in units of  $\chi_0 = 4\pi e^2 |t|^2 \mathcal{S} N(0)^2 \Delta_0$ . We assume that  $M_L(\omega) = M_R(\omega)$  and for the anomalous density of states we take the result for the two-mode model (3) shown in Fig. 2. Dotted lines show the energy scales  $2\Delta_0$ ,  $\Omega_\perp$  and  $\Omega_0$ . Note the logarithmic scale of  $\omega$ .

ume. This is a standard assumption for tunnel junctions with an oxide barrier [7], but it should apply also to scanning tunneling spectroscopy with a superconducting tip [9]. If we furthermore introduce the anomalous versions of the tunneling density of states for the left and right superconductors,  $M_L(\omega) = \frac{1}{V} \sum_{\mathbf{k}} B_{\mathbf{k}}(\omega)$  and  $M_R(\omega) = \frac{1}{V} \sum_{\mathbf{q}} B_{\mathbf{q}}(\omega)$ , then the function  $\chi''_{S0}(\omega)$  can be written as

$$\chi''_{S0}(\omega) = 4\pi e^2 |t|^2 \mathcal{S} \int_{-\infty}^{\infty} dx [f(x + \omega) - f(x)] M_L(x) M_R(x + \omega). \quad (13)$$

Since the critical current of the junction is given by  $I_c = \frac{1}{\pi e} \int_{-\infty}^{\infty} \frac{d\omega}{\omega} \chi''_{S0}(\omega)$ , the typical fluctuating current is  $\langle I^2 \rangle \sim \frac{\varepsilon}{\tau} I_c$ , where  $\tau$  is a typical fluctuation time defined by  $\chi''_{S0}(\omega)$ . Note that  $\langle I^2 \rangle$  scales with the junction area  $\mathcal{S}$ , as should have been expected.

We shall demonstrate the usefulness of equation (13) by applying it to the conventional low-temperature superconductors, in which case the functions  $Z$  and  $\Delta$  do not depend on momentum. From equation (2) it then follows that the anomalous density of states is

$$\frac{M(\omega)}{N(0)} = -\frac{1}{\pi} \int d\varepsilon_k \text{Im} F_{\mathbf{k}}(\omega + i0) = \text{Re} \frac{\text{sgn}(\omega) \Delta(\omega)}{\sqrt{\omega^2 - \Delta^2(\omega)}}. \quad (14)$$

Note the similarity of the result for  $M(\omega)$  to equation (7), in particular that neither  $M(\omega)$ , nor  $N_S(\omega)$  depend on the wave function renormalisation  $Z(\omega)$ . Therefore both functions can be used as a direct measure of  $\Delta(\omega)$ . An explicit example of the anomalous density of states for the two-mode model (3) is shown in Figure 2. Note that  $M(\omega)$  carries the same spectroscopic information as  $N_S(\omega)$ , but its spectroscopic features are (i) more pronounced and (ii) not masked by a large constant background  $N(0)$ .

In Figure 4 we plot the function  $\chi''_{S0}(\omega)$  for a junction formed by two identical superconductors described by the two-mode model (3). As expected, the pairing and pair-breaking scales are discriminated by  $\chi''_{S0}(\omega)$  in the same way as by  $M(\omega)$ .

Let us conclude by suggesting a two-step procedure for quantitative determination of the pairing glue from the measured function  $\chi''_{S0}(\omega)$ .

In the first step, equation (13) needs to be inverted and the function  $M(\omega)$  of the studied superconductor (say, the right one) has to be found. This task can be reduced to matrix inversion in the case when the function  $M_L(\omega)$  is known, i.e. when one of the superconductors forming the Josephson junction is well understood. Alternatively, in Appendix B we suggest a low-temperature inversion procedure for

the case when both sides of the junction are made of the studied superconductor.

In the second step, we should invert (14) to obtain the complex function  $\Delta(\omega)$ . It should be possible to perform this task by modifying the approach of [8].

## 5. Conclusions

To summarize, we have presented a short review of the techniques used to extract information on the pairing glue in superconductors, having in mind their applicability to the cuprates. All currently available experimental techniques exploit data on the normal spectral function  $A_{\mathbf{k}}(x)$ . The most promising approaches of this type have been described in Sections 3.2 and 3.3. Since all  $A_{\mathbf{k}}(x)$ -based techniques need to postulate that the normal and anomalous self-energies do not depend on  $\varepsilon_{\mathbf{k}}$  and since this assumption may not hold in the cuprates, in Section 4 we have suggested a novel technique for a direct measurement of the anomalous spectral function  $B_{\mathbf{k}}(x)$ , which makes use of the correlation function  $\chi(\omega)$  of currents in a Josephson junction involving the studied superconductor. This enables in principle a much more direct determination of the pairing glue in a superconductor, when compared to the conventional  $A_{\mathbf{k}}(x)$ -based techniques.

As a proof of concept, we have analyzed  $\chi(\omega)$  in junctions between conventional isotropic superconductors in the simplest case of featureless tunneling. Obviously, in order to be applicable to the cuprates, some degree of directionality of tunneling will need to be allowed for, since in a  $d$ -wave superconductor the anomalous density of states  $M(\omega)$  vanishes. Moreover, especially in junctions involving underdoped cuprates, the effect of phase fluctuations on  $\chi(\omega)$  may have to be included. The most pressing question, however, is how to measure  $\chi(\omega)$  at the (presumably) high typical frequencies of the pairing glue, when the complex conductivity of the junction is likely to be dominated by its capacitance.

Quite generally, irreducible correlation functions of other observables, such as charge-charge, spin-spin, etc., involve normal and superconducting contributions resembling (12). Unfortunately, their analysis is much more complicated than in the present case, because of the non-vanishing vertex corrections. Moreover, even in simplest cases the physical correlation functions are given as a geometric series of irreducible correlation functions. Nevertheless, it might be possible to extract  $B_{\mathbf{k}}(x)$  also from appropriate combinations of correlation functions which are more readily measurable than  $\chi(\omega)$ . Such approaches definitely deserve further study.

## Acknowledgement

This work was supported by the Slovak Research and Development Agency under Grant No. APVV-0558-10.

## References

- [1] C.C. Tsuei and J.R. Kirtley, Rev. Mod. Phys. 72 (2000) p. 969.
- [2] P.W. Anderson, Science 316 (2007) p. 1705.
- [3] G. Rickayzen, *Green's Functions and Condensed Matter*, Academic Press, London, 1980.
- [4] J.C. Campuzano, M.R. Norman and M. Randeria, *Photoemission in the High Tc Superconductors*, in *The Physics of Superconductors*, K.H. Bennemann and J.B. Ketterson, eds., Vol. II, Springer, New York, 2004, pp. 167-273.
- [5] S.R. Park, Y. Cao, Q. Wang, M. Fujita, K. Yamada, S.-K. Mo, D.S. Dessau and D. Reznik, Phys. Rev. B 88 (2013) art. no. 220503(R).
- [6] K.S.D. Beach, R.J. Gooding and F. Marsiglio, Phys. Rev. B 61 (2000) p. 5147.
- [7] J.R. Schrieffer, *Theory of Superconductivity*, Benjamin, New York, 1964.

- [8] A.A. Galkin, A.I. D'yachenko and V.M. Svistunov, Sov. Phys. JETP 39 (1974) p. 1115.
- [9] C. Berthod, Y. Fasano, I. Maggio-Aprile, A. Piriou, E. Giannini, G. Levy de Castro and Ø. Fischer, Phys. Rev. B 88 (2013) art. no. 014528.
- [10] T.J. Reber, N.C. Plumb, Z. Sun, Y. Cao, Q. Wang, K. McElroy, H. Iwasawa, M. Arita, J.S. Wen, Z.J. Xu, G. Gu, Y. Yoshida, H. Eisaki, Y. Aiura and D.S. Dessau, Nature Physics 8 (2012) p. 606.
- [11] T.J. Reber, N.C. Plumb, Y. Cao, Z. Sun, Q. Wang, K. McElroy, H. Iwasawa, M. Arita, J.S. Wen, Z.J. Xu, G. Gu, Y. Yoshida, H. Eisaki, Y. Aiura and D.S. Dessau, Phys. Rev. B 87 (2013) art. no. 060506.
- [12] W. Zhang, J.M. Bok, J.H. Yun, J. He, G. Liu, L. Zhao, H. Liu, J. Meng, X. Jia, Y. Peng, D. Mou, S. Liu, L. Yu, S. He, X. Dong, J. Zhang, J.S. Wen, Z.J. Xu, G.D. Gu, G. Wang, Y. Zhu, X. Wang, Q. Peng, Z. Wang, S. Zhang, F. Yang, C. Chen, Z. Xu, H.-Y. Choi, C.M. Varma and X.J. Zhou, Phys. Rev. B 85 (2012) art. no. 064514.
- [13] A. Pushp, C.V. Parker, A.N. Pasupathy, K.K. Gomes, S. Ono, J. Wen, Z. Xu, G. Gu and A. Yazdani, Science 324 (2009) p. 1689.

## Appendix A. Proof of the sum rule (5)

Because of the symmetry  $\phi_{\mathbf{k}}''(\omega) = -\phi_{\mathbf{k}}''(-\omega)$  of the anomalous self-energy  $\phi_{\mathbf{k}}(\omega) = Z_{\mathbf{k}}(\omega)\Delta_{\mathbf{k}}(\omega)$ , the Kramers-Kronig relations imply in the limit  $\omega \rightarrow \infty$  the scaling

$$\phi_{\mathbf{k}}'(\omega) - \phi_{\mathbf{k}}'(\infty) = \frac{1}{\pi} \int_{-\infty}^{\infty} \frac{dz \phi_{\mathbf{k}}''(z)}{z - \omega} \propto \frac{1}{\omega^2}.$$

Since in any dynamic theory without instantaneous interactions  $\phi_{\mathbf{k}}'(\infty) = 0$ , in the limit  $\omega \rightarrow \infty$  we therefore have  $\phi_{\mathbf{k}}'(\omega) \propto \frac{1}{\omega^2}$  and from equation (2) it follows that  $F_{\mathbf{k}}'(\omega) \propto \frac{1}{\omega^4}$ . On the other hand, the spectral representation (1) can be written at  $\omega \rightarrow \infty$  as a power series

$$F_{\mathbf{k}}'(\omega) = \sum_{n=0}^{\infty} \frac{1}{\omega^{n+1}} \int_{-\infty}^{\infty} dx x^n B_{\mathbf{k}}(x).$$

But because  $F_{\mathbf{k}}'(\omega) \propto \frac{1}{\omega^4}$ , the first three terms  $n = 0, 1, 2$  have to vanish. Since  $B_{\mathbf{k}}(x)$  is odd, the results for  $n = 0$  and  $2$  are trivial. On the other hand, the result for  $n = 1$  is the sum rule (5).

## Appendix B. Inversion of (13) in the case $M_L(x) = M_R(x)$

The functions  $\chi_{S_0}''(\omega)$  and  $M_L(\omega) = M_R(\omega) \equiv M(\omega)$  are antisymmetric, so they can be reconstructed from their values at  $\omega > 0$ . We therefore define  $\tilde{\chi}(\omega) = \chi_{S_0}''(\omega)\theta(\omega)$  and  $\tilde{M}(\omega) = M(\omega)\theta(\omega)$ , where  $\theta(\omega)$  is the step function. The crucial observation is that at zero temperature  $[f(x+\omega) - f(x)]\theta(\omega) = -\theta(-x)\theta(x+\omega)$ , and therefore

$$\tilde{\chi}(\omega) = 4e^2 |t|^2 \mathcal{S} \int_{-\infty}^{\infty} dx \tilde{M}(-x) \tilde{M}(x+\omega).$$

Since  $\tilde{\chi}(\omega)$  is a convolution, Fourier transformation to the time domain leads to  $\tilde{\chi}(t) \propto \tilde{M}^2(t)$ . The inversion of (13) is now straightforward. One first finds the Fourier transform  $\tilde{\chi}(t)$ , then takes the square root to obtain  $\tilde{M}(t)$ , Fourier transforms back to the frequency domain, and finally reconstructs  $M(\omega)$  from  $\tilde{M}(\omega)$ . The second step is subtle because the square root has two branches. The procedure is feasible only if  $\tilde{M}(t)$  is a *continuous* function that *never crosses zero*. However, the second condition fails only in very special cases, because  $\tilde{M}(t)$  is a complex-valued function.